Partial-wave analysis of $J/\psi \to K^+K^-\pi^0$

M. Ablikim,[1] M. N. Achasov,[10,d] P. Adlarson,[59] S. Ahmed,[15] M. Albrecht,[4] M. Alekseev,[58a,58c] A. Amoroso,[58a,58c] F. F. An,[1] Q. An,[55,43] Y. Bai,[42] O. Bakina,[27] R. Baldini Ferroli,[23a] I. Balossino,[24a] Y. Ban,[35] K. Begzsuren,[25] J. V. Bennett,[5] N. Berger,[26] M. Bertani,[23a] D. Bettoni,[24a] F. Bianchi,[58a,58c] J. Biernat,[59] J. Bloms,[52] I. Boyko,[27] R. A. Briere,[5] H. Cai,[60] X. Cai,[1,43] A. Calcaterra,[23a] G. F. Cao,[1,47] N. Cao,[1,47] S. A. Cetin,[46b] J. Chai,[58c] J. F. Chang,[1,43] W. L. Chang,[1,47] G. Chelkov,[27,b,c] D. Y. Chen,[6] G. Chen,[1] H. S. Chen,[1,47] J. C. Chen,[1] M. L. Chen,[1,43] S. J. Chen,[33] Y. B. Chen,[1,43] W. Cheng,[58c] G. Cibinetto,[24a] F. Cossio,[58c] X. F. Cui,[34] H. L. Dai,[1,43] J. P. Dai,[38,h] X. C. Dai,[1,47] A. Dbeyssi,[15] D. Dedovich,[27] Z. Y. Deng,[1] A. Denig,[26] I. Denysenko,[27,*] M. Destefanis,[58a,58c] F. De Mori,[58a,58c] Y. Ding,[31] C. Dong,[34] J. Dong,[1,43] L. Y. Dong,[1,47] M. Y. Dong,[1,43,47] Z. L. Dou,[33] S. X. Du,[63] J. Z. Fan,[45] J. Fang,[1,43] S. S. Fang,[1,47] Y. Fang,[1] R. Farinelli,[24a,24b] L. Fava,[58b,58c] F. Feldbauer,[4] G. Felici,[23a] C. Q. Feng,[55,43] M. Fritsch,[4] C. D. Fu,[1] Y. Fu,[1] Q. Gao,[1] X. L. Gao,[55,43] Y. Gao,[45] Y. Gao,[56] Y. G. Gao,[6] Z. Gao,[55,43] B. Garillon,[26] I. Garzia,[24a] E. M. Gersabeck,[50] A. Gilman,[51] K. Goetzen,[11] L. Gong,[34] W. X. Gong,[1,43] W. Gradl,[26] M. Greco,[58a,58c] L. M. Gu,[33] M. H. Gu,[1,43] S. Gu,[2] Y. T. Gu,[13] A. Q. Guo,[22] L. B. Guo,[32] R. P. Guo,[36] Y. P. Guo,[26] A. Guskov,[27] S. Han,[60] X. Q. Hao,[16] F. A. Harris,[48] K. L. He,[1,47] F. H. Heinsius,[4] T. Held,[4] Y. K. Heng,[1,43,47] M. Himmelreich,[11,g] Y. R. Hou,[47] Z. L. Hou,[1] H. M. Hu,[1,47] J. F. Hu,[38,h] T. Hu,[1,43,47] Y. Hu,[1] G. S. Huang,[55,43] J. S. Huang,[16] X. T. Huang,[37] X. Z. Huang,[33] N. Huesken,[52] T. Hussain,[57] W. Ikegami Andersson,[59] W. Imoehl,[22] M. Irshad,[55,43] Q. Ji,[1] Q. P. Ji,[16] X. B. Ji,[1,47] X. L. Ji,[1,43] H. L. Jiang,[37] X. S. Jiang,[1,43,47] X. Y. Jiang,[34] J. B. Jiao,[37] Z. Jiao,[18] D. P. Jin,[1,43,47] S. Jin,[33] Y. Jin,[49] T. Johansson,[59] N. Kalantar-Nayestanaki,[29] X. S. Kang,[31] R. Kappert,[29] M. Kavatsyuk,[29] B. C. Ke,[1] I. K. Keshk,[4] A. Khoukaz,[52] P. Kiese,[26] R. Kiuchi,[1] R. Kliemt,[11] L. Koch,[28] O. B. Kolcu,[46b,f] B. Kopf,[4] M. Kuemmel,[4] M. Kuessner,[4] A. Kupsc,[59] M. Kurth,[1] M. G. Kurth,[1,47] W. Kühn,[28] J. S. Lange,[28] P. Larin,[15] L. Lavezzi,[58c] H. Leithoff,[26] T. Lenz,[26] C. Li,[59] Cheng Li,[55,43] D. M. Li,[63] F. Li,[1,43] F. Y. Li,[35] G. Li,[1] H. B. Li,[1,47] H. J. Li,[9,j] J. C. Li,[1] J. W. Li,[41] Ke Li,[1] L. K. Li,[1] Lei Li,[3] P. L. Li,[55,43] P. R. Li,[30] Q. Y. Li,[37] W. D. Li,[1,47] W. G. Li,[1] X. H. Li,[55,43] X. L. Li,[37] X. N. Li,[1,43] Z. B. Li,[44] Z. Y. Li,[44] H. Liang,[55,43] H. Liang,[1,47] Y. F. Liang,[40] Y. T. Liang,[28] G. R. Liao,[12] L. Z. Liao,[1,47] J. Libby,[21] C. X. Lin,[44] D. X. Lin,[15] Y. J. Lin,[13] B. Liu,[38,h] B. J. Liu,[1] C. X. Liu,[1] D. Liu,[55,43] D. Y. Liu,[38,h] F. H. Liu,[39] Fang Liu,[1] Feng Liu,[6] H. B. Liu,[13] H. M. Liu,[1,47] Huanhuan Liu,[1] Huihui Liu,[17] J. B. Liu,[55,43] J. Y. Liu,[1,47] K. Y. Liu,[31] Ke Liu,[6] L. Y. Liu,[13] Q. Liu,[47] S. B. Liu,[55,43] T. Liu,[1,47] X. Liu,[30] X. Y. Liu,[1,47] Y. B. Liu,[34] Z. A. Liu,[1,43,47] Zhiqing Liu,[37] Y. F. Long,[35] X. C. Lou,[1,43,47] H. J. Lu,[18] J. D. Lu,[1,47] J. G. Lu,[1,43] Y. Lu,[1] Y. P. Lu,[1,43] C. L. Luo,[32] M. X. Luo,[62] P. W. Luo,[44] T. Luo,[9,j] X. L. Luo,[1,43] S. Lusso,[58c] X. R. Lyu,[47] F. C. Ma,[31] H. L. Ma,[1] L. L. Ma,[37] M. M. Ma,[1,47] Q. M. Ma,[1] X. N. Ma,[34] X. X. Ma,[1,47] X. Y. Ma,[1,43] Y. M. Ma,[37] F. E. Maas,[15] M. Maggiora,[58a,58c] S. Maldaner,[26] S. Malde,[53] Q. A. Malik,[57] A. Mangoni,[23b] Y. J. Mao,[35] Z. P. Mao,[1] S. Marcello,[58a,58c] Z. X. Meng,[49] J. G. Messchendorp,[29] G. Mezzadri,[24a] J. Min,[1,43] T. J. Min,[33] R. E. Mitchell,[22] X. H. Mo,[1,43,47] Y. J. Mo,[6] C. Morales Morales,[15] N. Yu. Muchnoi,[10,d] H. Muramatsu,[51] A. Mustafa,[4] S. Nakhoul,[11,g] Y. Nefedov,[27] F. Nerling,[11,g] I. B. Nikolaev,[10,d] Z. Ning,[1,43] S. Nisar,[8,k] S. L. Niu,[1,43] S. L. Olsen,[47] Q. Ouyang,[1,43,47] S. Pacetti,[23b] Y. Pan,[55,43] M. Papenbrock,[59] P. Patteri,[23a] M. Pelizaeus,[4] H. P. Peng,[55,43] K. Peters,[11,g] J. Pettersson,[59] J. L. Ping,[32] R. G. Ping,[1,47] A. Pitka,[4] R. Poling,[51] V. Prasad,[55,43] H. R. Qi,[2] M. Qi,[33] T. Y. Qi,[2] S. Qian,[1,43] C. F. Qiao,[47] N. Qin,[60] X. P. Qin,[13] X. S. Qin,[4] Z. H. Qin,[1,43] J. F. Qiu,[1] S. Q. Qu,[34] K. H. Rashid,[57,i] K. Ravindran,[21] C. F. Redmer,[26] M. Richter,[4] A. Rivetti,[58c] V. Rodin,[29] M. Rolo,[58c] G. Rong,[1,47] Ch. Rosner,[15] M. Rump,[52] A. Sarantsev,[27,e] M. Savrié,[24b] Y. Schelhaas,[26] K. Schoenning,[59] W. Shan,[19] X. Y. Shan,[55,43] M. Shao,[55,43] C. P. Shen,[2] P. X. Shen,[34] X. Y. Shen,[1,47] H. Y. Sheng,[1] X. Shi,[1,43] X. D. Shi,[55,43] J. J. Song,[37] Q. Q. Song,[55,43] X. Y. Song,[1] S. Sosio,[58a,58c] C. Sowa,[4] S. Spataro,[58a,58c] F. F. Sui,[37] G. X. Sun,[1] J. F. Sun,[16] L. Sun,[60] S. S. Sun,[1,47] X. H. Sun,[1] Y. J. Sun,[55,43] Y. K. Sun,[55,43] Y. Z. Sun,[1] Z. J. Sun,[1,43] Z. T. Sun,[1] Y. T. Tan,[55,43] C. J. Tang,[40] G. Y. Tang,[1] X. Tang,[1] V. Thoren,[59] B. Tsednee,[25] I. Uman,[46d] B. Wang,[1] B. L. Wang,[47] C. W. Wang,[33] D. Y. Wang,[35] K. Wang,[1,43] L. L. Wang,[1] L. S. Wang,[1] M. Wang,[37] M. Z. Wang,[35] Meng Wang,[1,47] P. L. Wang,[1] R. M. Wang,[61] W. P. Wang,[55,43] X. Wang,[35] X. F. Wang,[1] X. L. Wang,[9,j] Y. Wang,[55,43] Y. Wang,[44] Y. F. Wang,[1,43,47] Z. Wang,[1,43] Z. G. Wang,[1,43] Z. Y. Wang,[1] Zongyuan Wang,[1,47] T. Weber,[4] D. H. Wei,[12] P. Weidenkaff,[26] H. W. Wen,[32] S. P. Wen,[1] U. Wiedner,[4] G. Wilkinson,[53] M. Wolke,[59] L. H. Wu,[1] L. J. Wu,[1,47] Z. Wu,[1,43] L. Xia,[55,43] Y. Xia,[20] S. Y. Xiao,[1] Y. J. Xiao,[1,47] Z. J. Xiao,[32] Y. G. Xie,[1,43] Y. H. Xie,[6] T. Y. Xing,[1,47] X. A. Xiong,[1,47] Q. L. Xiu,[1,43] G. F. Xu,[1] J. J. Xu,[33] L. Xu,[1] Q. J. Xu,[14] W. Xu,[1,47] X. P. Xu,[41] F. Yan,[56] L. Yan,[58a,58c] W. B. Yan,[55,43] W. C. Yan,[2] Y. H. Yan,[20] H. J. Yang,[38,h] H. X. Yang,[1] L. Yang,[60] R. X. Yang,[55,43] S. L. Yang,[1,47] Y. H. Yang,[33] Y. X. Yang,[12] Yifan Yang,[1,47] Z. Q. Yang,[20] M. Ye,[1,43] M. H. Ye,[7] J. H. Yin,[1] Z. Y. You,[44] B. X. Yu,[1,43,47] C. X. Yu,[34] J. S. Yu,[20] T. Yu,[56] C. Z. Yuan,[1,47] X. Q. Yuan,[35] Y. Yuan,[1] A. Yuncu,[46b,a] A. A. Zafar,[57] Y. Zeng,[20] B. X. Zhang,[1] B. Y. Zhang,[1,43] C. C. Zhang,[1] D. H. Zhang,[1] H. H. Zhang,[44] H. Y. Zhang,[1,43] J. Zhang,[1,47] J. L. Zhang,[61] J. Q. Zhang,[4] J. W. Zhang,[1,43,47] J. Y. Zhang,[1] J. Z. Zhang,[1,47] K. Zhang,[1,47] L. Zhang,[45] S. F. Zhang,[33] T. J. Zhang,[38,h] X. Y. Zhang,[37] Y. Zhang,[55,43] Y. H. Zhang,[1,43] Y. T. Zhang,[55,43] Yang Zhang,[1] Yao Zhang,[1] Yi Zhang,[9,j] Yu Zhang,[47] Z. H. Zhang,[6] Z. P. Zhang,[55] Z. Y. Zhang,[60] G. Zhao,[1] J. W. Zhao,[1,43] J. Y. Zhao,[1,47]

J. Z. Zhao,[1,43] Lei Zhao,[55,43] Ling Zhao,[1] M. G. Zhao,[34] Q. Zhao,[1] S. J. Zhao,[63] T. C. Zhao,[1] Y. B. Zhao,[1,43] Z. G. Zhao,[55,43] A. Zhemchugov,[27,b] B. Zheng,[56] J. P. Zheng,[1,43] Y. Zheng,[35] Y. H. Zheng,[47] B. Zhong,[32] L. Zhou,[1,43] L. P. Zhou,[1,47] Q. Zhou,[1,47] X. Zhou,[60] X. K. Zhou,[47] X. R. Zhou,[55,43] Xiaoyu Zhou,[20] Xu Zhou,[20] A. N. Zhu,[1,47] J. Zhu,[34] J. Zhu,[44] K. Zhu,[1] K. J. Zhu,[1,43,47] S. H. Zhu,[54] W. J. Zhu,[34] X. L. Zhu,[45] Y. C. Zhu,[55,43] Y. S. Zhu,[1,47] Z. A. Zhu,[1,47] J. Zhuang,[1,43] B. S. Zou,[1] and J. H. Zou[1]

(BESIII Collaboration)

[1]*Institute of High Energy Physics, Beijing 100049, People's Republic of China*
[2]*Beihang University, Beijing 100191, People's Republic of China*
[3]*Beijing Institute of Petrochemical Technology, Beijing 102617, People's Republic of China*
[4]*Bochum Ruhr-University, D-44780 Bochum, Germany*
[5]*Carnegie Mellon University, Pittsburgh, Pennsylvania 15213, USA*
[6]*Central China Normal University, Wuhan 430079, People's Republic of China*
[7]*China Center of Advanced Science and Technology, Beijing 100190, People's Republic of China*
[8]*COMSATS University Islamabad, Lahore Campus, Defence Road, Off Raiwind Road, 54000 Lahore, Pakistan*
[9]*Fudan University, Shanghai 200443, People's Republic of China*
[10]*G.I. Budker Institute of Nuclear Physics SB RAS (BINP), Novosibirsk 630090, Russia*
[11]*GSI Helmholtzcentre for Heavy Ion Research GmbH, D-64291 Darmstadt, Germany*
[12]*Guangxi Normal University, Guilin 541004, People's Republic of China*
[13]*Guangxi University, Nanning 530004, People's Republic of China*
[14]*Hangzhou Normal University, Hangzhou 310036, People's Republic of China*
[15]*Helmholtz Institute Mainz, Johann-Joachim-Becher-Weg 45, D-55099 Mainz, Germany*
[16]*Henan Normal University, Xinxiang 453007, People's Republic of China*
[17]*Henan University of Science and Technology, Luoyang 471003, People's Republic of China*
[18]*Huangshan College, Huangshan 245000, People's Republic of China*
[19]*Hunan Normal University, Changsha 410081, People's Republic of China*
[20]*Hunan University, Changsha 410082, People's Republic of China*
[21]*Indian Institute of Technology Madras, Chennai 600036, India*
[22]*Indiana University, Bloomington, Indiana 47405, USA*
[23a]*INFN Laboratori Nazionali di Frascati, I-00044 Frascati, Italy*
[23b]*INFN and University of Perugia, I-06100 Perugia, Italy*
[24a]*INFN Sezione di Ferrara, I-44122 Ferrara, Italy*
[24b]*University of Ferrara, I-44122 Ferrara, Italy*
[25]*Institute of Physics and Technology, Peace Avenue 54B, Ulaanbaatar 13330, Mongolia*
[26]*Johannes Gutenberg University of Mainz, Johann-Joachim-Becher-Weg 45, D-55099 Mainz, Germany*
[27]*Joint Institute for Nuclear Research, 141980 Dubna, Moscow Region, Russia*
[28]*Justus-Liebig-Universitaet Giessen, II. Physikalisches Institut, Heinrich-Buff-Ring 16, D-35392 Giessen, Germany*
[29]*KVI-CART, University of Groningen, NL-9747 AA Groningen, Netherlands*
[30]*Lanzhou University, Lanzhou 730000, People's Republic of China*
[31]*Liaoning University, Shenyang 110036, People's Republic of China*
[32]*Nanjing Normal University, Nanjing 210023, People's Republic of China*
[33]*Nanjing University, Nanjing 210093, People's Republic of China*
[34]*Nankai University, Tianjin 300071, People's Republic of China*
[35]*Peking University, Beijing 100871, People's Republic of China*
[36]*Shandong Normal University, Jinan 250014, People's Republic of China*
[37]*Shandong University, Jinan 250100, People's Republic of China*
[38]*Shanghai Jiao Tong University, Shanghai 200240, People's Republic of China*
[39]*Shanxi University, Taiyuan 030006, People's Republic of China*
[40]*Sichuan University, Chengdu 610064, People's Republic of China*
[41]*Soochow University, Suzhou 215006, People's Republic of China*
[42]*Southeast University, Nanjing 211100, People's Republic of China*
[43]*State Key Laboratory of Particle Detection and Electronics, Beijing 100049, Hefei 230026, People's Republic of China*
[44]*Sun Yat-Sen University, Guangzhou 510275, People's Republic of China*
[45]*Tsinghua University, Beijing 100084, People's Republic of China*
[46a]*Ankara University, 06100 Tandogan, Ankara, Turkey*
[46b]*Istanbul Bilgi University, 34060 Eyup, Istanbul, Turkey*

[46c]Uludag University, 16059 Bursa, Turkey
[46d]Near East University, Nicosia, North Cyprus, Mersin 10, Turkey
[47]University of Chinese Academy of Sciences, Beijing 100049, People's Republic of China
[48]University of Hawaii, Honolulu, Hawaii 96822, USA
[49]University of Jinan, Jinan 250022, People's Republic of China
[50]University of Manchester, Oxford Road, Manchester M13 9PL, United Kingdom
[51]University of Minnesota, Minneapolis, Minnesota 55455, USA
[52]University of Muenster, Wilhelm-Klemm-Street 9, 48149 Muenster, Germany
[53]University of Oxford, Keble Road, Oxford, United Kingdom OX13RH, United Kingdom
[54]University of Science and Technology Liaoning, Anshan 114051, People's Republic of China
[55]University of Science and Technology of China, Hefei 230026, People's Republic of China
[56]University of South China, Hengyang 421001, People's Republic of China
[57]University of the Punjab, Lahore-54590, Pakistan
[58a]University of Turin, I-10125 Turin, Italy
[58b]University of Eastern Piedmont, I-15121 Alessandria, Italy
[58c]INFN, I-10125 Turin, Italy
[59]Uppsala University, Box 516, SE-75120 Uppsala, Sweden
[60]Wuhan University, Wuhan 430072, People's Republic of China
[61]Xinyang Normal University, Xinyang 464000, People's Republic of China
[62]Zhejiang University, Hangzhou 310027, People's Republic of China
[63]Zhengzhou University, Zhengzhou 450001, People's Republic of China

(Received 25 April 2019; published 14 August 2019)

A partial-wave analysis of the decay $J/\psi \to K^+K^-\pi^0$ has been made using $(223.7 \pm 1.4) \times 10^6$ J/ψ events collected with the BESIII detector in 2009. The analysis, which is performed within the isobar-model approach, reveals contributions from $K_2^*(1430)^\pm$, $K_2^*(1980)^\pm$ and $K_4^*(2045)^\pm$ decaying to $K^\pm\pi^0$. The two latter states are observed in J/ψ decays for the first time. Two resonance signals decaying to K^+K^- are also observed. These contributions cannot be reliably identified and their possible interpretations are discussed. The measured branching fraction $B(J/\psi \to K^+K^-\pi^0)$ of $(2.88 \pm 0.01 \pm 0.12) \times 10^{-3}$ is more precise than previous results. Branching fractions for the reported contributions are presented as well. The results of the partial-wave analysis differ significantly from those previously obtained by BESII and *BABAR*.

DOI: 10.1103/PhysRevD.100.032004

I. INTRODUCTION

A good knowledge of the spectrum and properties of hadrons is one of the key issues for understanding the strong interaction at low and intermediate energies. The conventional quark model implies that quark-antiquark states are produced as nonets, which consist of mesons with strange and nonstrange quarks. Therefore, an accurate identification of mesons with one strange quark can help to

*Corresponding author.
iden@jinr.ru
[a]Also at Bogazici University, 34342 Istanbul, Turkey.
[b]Also at the Moscow Institute of Physics and Technology, Moscow 141700, Russia.
[c]Also at the Functional Electronics Laboratory, Tomsk State University, Tomsk, 634050, Russia.
[d]Also at the Novosibirsk State University, Novosibirsk, 630090, Russia.
[e]Also at the NRC "Kurchatov Institute", PNPI, 188300, Gatchina, Russia.
[f]Also at Istanbul Arel University, 34295 Istanbul, Turkey.
[g]Also at Goethe University Frankfurt, 60323 Frankfurt am Main, Germany.
[h]Also at Key Laboratory for Particle Physics, Astrophysics and Cosmology, Ministry of Education; Shanghai Key Laboratory for Particle Physics and Cosmology; Institute of Nuclear and Particle Physics, Shanghai 200240, People's Republic of China.
[i]Also at Government College Women University, Sialkot—51310, Punjab, Pakistan.
[j]Also at Key Laboratory of Nuclear Physics and Ion-beam Application (MOE) and Institute of Modern Physics, Fudan University, Shanghai 200443, People's Republic of China.
[k]Also at Harvard University, Department of Physics, Cambridge, Massachusetts 02138, USA.

establish nonet members in the isoscalar sector, where the situation is more complicated. This is due to a potential mixing between octet and singlet states as well as possible mixing with glueball states.

The identification of meson radial excitations also helps in the understanding of quark-antiquark interaction at intermediate energies. Quark potential models [1] predict that the squared masses of radial excitations depend on the excitation number quadratically. However, in the analysis of proton-antiproton annihilation in flight, it was found that this dependence is close to the linear one similar to the Regge trajectories [2]. If correct, this behavior has the potential to reveal a new symmetry of the quark-antiquark interaction [3,4]. Therefore, the experimental confirmation (or disproof) of this behavior is an important task in experimental hadron physics.

J/ψ decays are ideal for the study of meson spectra and the determination of meson properties. They can provide important information about meson states with masses up to 3 GeV/c^2 and partial-wave analysis is facilitated due to the well-known quantum numbers of the initial state. Moreover, the J/ψ radiative decay is favored for the production of glueball states which makes it a perfect tool to search for and study such exotics [5].

In this paper we report the results of a partial-wave analysis (PWA) of the decay $J/\psi \to K^+K^-\pi^0$. This decay channel has been previously studied by the MARK [6], MARK-II [7], MARK-III [8], DM2 [9], BESII [10], and *BABAR* [11,12] collaborations, but only two recent publications report PWA results. In the first of these [10], BESII analyzes 58 million J/ψ decays and observes a very broad exotic resonance $X(1575) \to K^+K^-$ with pole position $[(1576^{+49+98}_{-55-91}) - i(409^{+11+32}_{-12-67})]$ MeV/c^2 and branching fraction $B(J/\psi \to X(1575)\pi^0 \to K^+K^-\pi^0) = (8.5 \pm 0.6^{+2.7}_{-3.6}) \times 10^{-4}$. In the second analysis [12], *BABAR* reports a PWA solution based on a smaller data set of 2102 events, which consists of $K^*(892)^{\pm}$, $K^*(1410)^{\pm}$ and $K_2^*(1430)^{\pm}$ states in the $K^{\pm}\pi^0$ channels, while the enhancement at low K^+K^- invariant masses is attributed to the $\rho(1450)$. The analysis presented in this paper is based on a data set of 182,972 event candidates selected from $(223.7 \pm 1.4) \times 10^6$ J/ψ decays [13] collected by the BESIII experiment in 2009. The high statistics and good data quality allow us to reveal signals from states that have not been observed before and precisely determine properties of intermediate states. Moreover, the obtained PWA solution can be used for the simulation of the irreducible background from this channel to the $J/\psi \to \gamma K^+K^-$ decay, which is one of the key channels to be studied in the search for a low-mass glueball.

II. BESIII EXPERIMENTAL FACILITY

The BESIII detector is a magnetic spectrometer [14] located at the Beijing Electron Positron Collider (BEPCII) [15]. The cylindrical core of the BESIII detector consists of a helium-based multilayer drift chamber (MDC), a plastic scintillator time-of-flight system (TOF), and a CsI(Tl) electromagnetic calorimeter (EMC), which are all enclosed in a superconducting solenoidal magnet providing a 1.0 T magnetic field. The solenoid is supported by an octagonal flux-return yoke with resistive plate counter muon identifier modules interleaved with steel. The geometrical acceptance of charged particles and photons is 93% over the 4π solid angle. The charged-particle momentum resolution at 1 GeV/c is 0.5%, and the dE/dx resolution is 6% for electrons from Bhabha scattering. The EMC measures photon energies with a resolution of 2.5% (5%) at 1 GeV in the barrel (end cap) region. The time resolution of the TOF barrel part is 68 ps, while that of the end-cap part is 110 ps.

The GEANT4-based simulation software BOOST [16] is used to simulate the detector response. An inclusive J/ψ Monte Carlo (MC) sample is used to estimate the background. In this sample the production of the J/ψ resonance is simulated by the MC event generator KKMC [17,18] and decays are generated by EVTGEN [19,20]. The branching fractions of known decay modes are set to the Particle Data Group (PDG) [21] world-average values and the remaining unknown decays are generated according to the Lund-Charm model [22].

III. EVENT SELECTION

The $K^+K^-\pi^0$ candidate events are required to have two charged tracks with zero net charge and at least two good photons.

Charged tracks must be reconstructed within the geometrical acceptance of the detector ($|\cos\theta| < 0.93$, where θ is the angle with respect to the beam axis) and originate from the interaction point ($|z| < 10$ cm and $R < 1$ cm, where z and R are minimal distances from a track to the run-averaged interaction point along the beam direction and in the transverse plane, respectively). An event is rejected if the transverse momentum of at least one charged track is too low ($p_T < 120$ MeV/c). Particle identification (PID) is performed using TOF and MDC dE/dx information. Their measurements are combined to form particle identification confidence levels (C.L.) for π, K, and p hypotheses, and the particle type with the highest C.L. is assigned to the track. Both tracks are required to be identified as kaons.

Signal clusters in the EMC within the acceptance region, which are not associated with charged tracks and possess energy $E > 25$ MeV in the barrel part of the detector and $E > 50$ MeV in the end caps, are treated as photon candidates. To exclude showers from association with charged particles, the angle between the shower direction and the charged tracks extrapolated to the EMC must be greater than 10 degrees. The requirement on the EMC cluster time with respect to the start of the event (0 ns $\leq t \leq$ 700 ns) is used to reject electronic noise and energy deposits not related to the analyzed event.

Consistency between the detector response and a final-state hypothesis (for the signal and specific background decays) is evaluated by a four-momentum constrained (4C) kinematic fit. Firstly, the accepted pair of charged tracks and each pair of the selected photon candidates with invariant mass $M_{\gamma\gamma} < 300\ \mathrm{MeV}/c^2$ are fitted under the $\gamma\gamma K^+K^-$ hypothesis. A combination with the lowest value of $\chi^2_{(4C)\gamma\gamma K^+K^-}$ is selected and an event is retained if $\chi^2_{(4C)\gamma\gamma K^+K^-} < 60$. Secondly, the $\chi^2_{(4C)\gamma\gamma K^+K^-}$ is compared to the corresponding value obtained in the best fits under the main background hypotheses: $\gamma\gamma\pi^+\pi^-$; γK^+K^-; and, in the cases in which more than two good photon candidates are selected, $\gamma\gamma\gamma K^+K^-$. If any of the background hypotheses results in a lower χ^2 value, the event is rejected. Finally, the π^0 candidates are reconstructed requiring the two-photon mass of the selected pair to be within a $110\ \mathrm{MeV}/c^2 < M_{\gamma\gamma} < 150\ \mathrm{MeV}/c^2$ interval. For the partial-wave analysis, we use particle momenta after the five-constrained (5C) kinematic fit, which also constrains the invariant mass of the selected photon pair to the nominal π^0 mass.

A total of 182,972 candidates satisfy the selection criteria. The corresponding number of background events is estimated from the inclusive MC: $N_{bg} = 565 \pm 24$ (or 0.3%). The largest background contributions come from the decay channels $J/\psi \to \gamma\eta_c, \eta_c \to K^+K^-\pi^0$ and $J/\psi \to \gamma K^+K^-$. The continuum background, i.e. that due to the $e^+e^- \to \gamma^* \to K^+K^-\pi^0$ process, is estimated from the analysis of a data sample of approximately 280 nb^{-1} collected from e^+e^- collisions at 3.08 GeV. It gives $N_{\mathrm{continuum}} = 855 \pm 499$, where the uncertainty is statistical. The background treatment in the PWA will be described in the next section.

The Dalitz plot for the selected data is shown in Fig. 1(a). Its most striking feature is a clear $K^*(892)^\pm$ signal. In the internal region of the plot a clear signal from $K_2^*(1430)^\pm$ is seen as well as structures at $M^2(K^\pm\pi^0) \approx 4\ \mathrm{GeV}^2/c^4$.

IV. PARTIAL-WAVE ANALYSIS

We use the isobar model to describe the J/ψ decay into $K^+K^-\pi^0$. The amplitude is parametrized as a sum of sequential quasi-two-body decay processes in this approach. The subprocess described by intermediate state production and the subsequent decay to a specific pair of the final-state mesons is referred to as the decay kinematic channel. The angular-dependent parts of the partial-wave amplitudes are calculated in the framework of the covariant tensor approach as described in detail in Ref. [23]. Note that in our case the conservation of P- and C-parities restricts the number of allowed partial waves for production and decay of any resonance to 1. To account for the finite size of

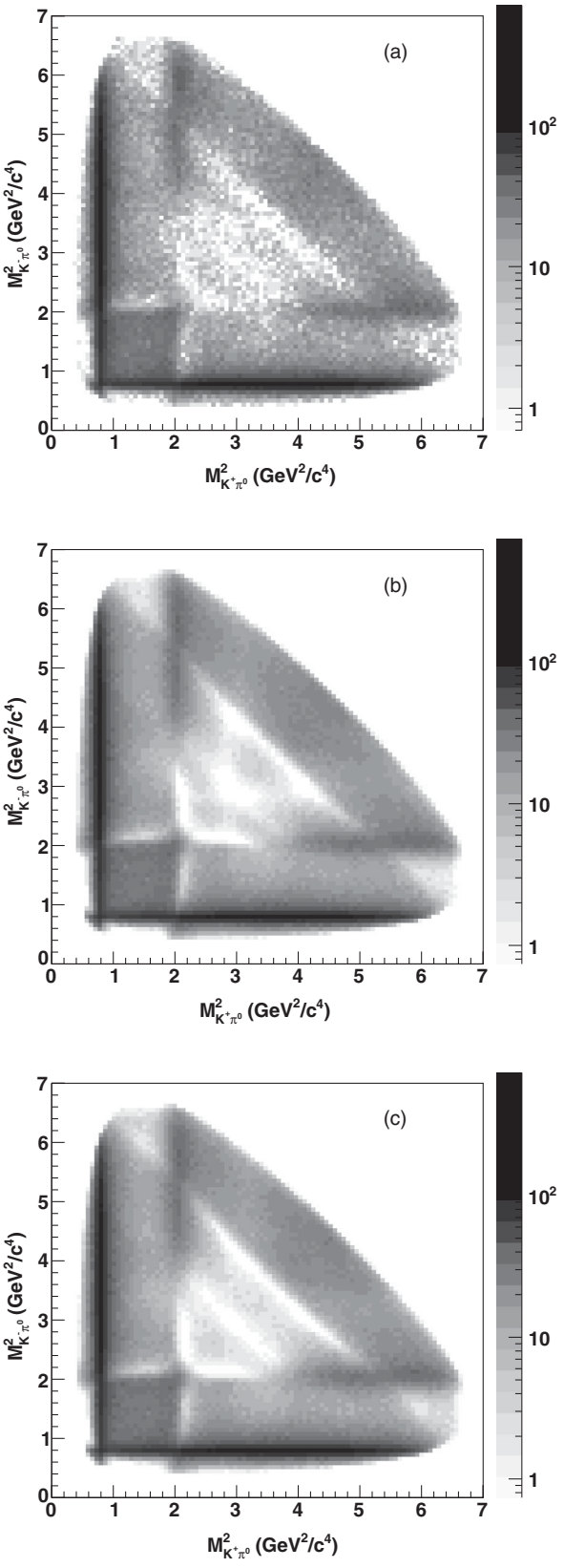

FIG. 1. Dalitz plots for the selected data (a), the PWA solution I (b) and the PWA solution II (c).

a hadron each decay vertex also includes Blatt-Weisskopf form factors, which depend on the Blatt-Weisskopf radius r. The Breit-Wigner term for the resonance a in the kinematic channel m (labeled by the number of the spectator particle) is

$$A^{BW}_{m,a} = \frac{1}{M_a^2 - s_m - iM_a\Gamma(s_m, J_a)}.$$

Here M_a, J_a and s_m are the resonance mass, spin and the invariant mass squared of its daughter particles, respectively. The width of the $K^*(892)^{\pm}$ state is defined by its decay to $K\pi$ and is parametrized as

$$\Gamma(s_m, J_a) = \frac{\rho_J(s_m)}{\rho_J(M_a^2)}\Gamma_a,$$
$$\rho_J(s_m) = \frac{2q}{\sqrt{s_m}}\frac{q^{2J}}{F^2(q^2, r, J)}. \quad (1)$$

Here, Γ_a is the resonance width; q is the relative momentum of the daughter particles calculated in the resonance rest frame; and $F(q^2, r, J)$ is the above-mentioned Blatt-Weisskopf form factor. The same parametrization is used for the width of the $K_2^*(1430)^{\pm}$ resonance, whose decay branching fraction to $K\pi$ is about 0.5. For other states we use a constant width $\Gamma(s_m, J_a) = \Gamma_a$ due to a small known branching fraction to the considered kinematic channel or due to the absence of reliable information about it.

The masses, widths, and decay radii [for the J/ψ, $K^*(892)^{\pm}$ and $K_2^*(1430)^{\pm}$] of resonances as well as the product of their production and decay couplings (complex numbers in general case) are initially free parameters of our fit. We find fit results weakly sensitive to the J/ψ decay radius. Hence, we set this parameter to be 0.7 fm, as is obtained in Ref. [24].

The analysis is performed within the framework of the event-by-event maximum likelihood method, which allows us to take into account all correlations in the multidimensional phase space. The negative log-likelihood function NLL is expressed as

$$\mathrm{NLL} = -\sum_i \ln\frac{\omega_i\epsilon_i}{\int \epsilon\omega d\Phi} = -\sum_i \ln\frac{\omega_i}{\int \epsilon\omega d\Phi} + \mathrm{const} \quad (2)$$

and is minimized. Here index i runs over the selected data events, ω_i is the decay-amplitude squared, summed over transverse J/ψ polarizations and evaluated from the four-momenta of final particles in the event i. The detector and event selection efficiency for the measured four-momenta is denoted by ϵ_i, the denominator is a normalization integral over the phase space (Φ), and the *const* term is independent of the fit parameters. The normalization integral is calculated using phase-space distributed MC events that pass the detector simulation and the event reconstruction. To take the background into account we estimate its contribution to the NLL function and subtract it. This is done by the evaluation of the NLL function over properly normalized data samples that have a kinematic distribution similar to that of the background. We consider two types of background channels: those producing a peak at the π^0 mass in the two-photon invariant-mass distribution ("peaking" background) and those exhibiting a smooth shape below the peak ("nonpeaking" background). The former is estimated from $J/\psi \to \gamma\eta_c$, $\eta_c \to \gamma K^+K^-\pi^0$ events selected under criteria similar to ones of the main event selection, and the latter is estimated from the π^0 mass cut sideband: 190 MeV/$c^2 < M_{\gamma\gamma} <$ 230 MeV/c^2.

This approach neglects the detector resolution, which is a good approximation for all resonances except for the $K^*(892)^{\pm}$. The MC simulation shows that estimated bias to the measured width of $K^*(892)^{\pm}$ is much larger than the corresponding systematic uncertainty estimated from other sources. At the same time, this bias is much smaller than the $K^*(892)^{\pm}$ width, which allows us to use the approximation proposed in Ref. [25] to take into account the detector resolution. Due to the significant computation time, this method is used only to correct the final PWA results.

The quality and consistency of the obtained solution is evaluated by the comparison of the mass and angular distributions of the experimental data and reconstructed phase-space generated MC events weighted according to the PWA solution.

The conservation of P- and C-parities strongly restricts the allowed quantum numbers of intermediate states. In the $K^{\pm}\pi^0$ channels only resonances with quantum numbers $I = 1/2$, $J^P = 1^-, 2^+, 3^-, 4^+\ldots$ can be produced. The reaction is dominated by $K^*(892)^{\pm}$ production. There are two other established vector states which are in the accessible mass region: $K^*(1410)$ and $K^*(1680)$ [26]. In the 2^+, 3^- and 4^+ partial waves three states are well established: $K_2^*(1430)$, $K_3^*(1780)$ and $K_4^*(2045)$. Possible contributions must also be considered from two observations reported by the LASS Collaboration: a 2^+ state at 1980 MeV/c^2 [27] (also claimed to be seen by SPEC [28]) and a 5^- state at 2380 MeV/c^2 [29], which needs confirmation. As for the K^+K^- channel, the produced resonances are restricted to quantum numbers $J^{PC} = J^{--}$, where $J = 1, 3, 5\ldots$ For the strong decays of the J/ψ isospin and G-parity conservation requires $I^G = 1^+$. There are two well-known isovector resonances in the $J^{PC} = 1^{--}$ sector, the $\rho(1450)$ and $\rho(1700)$, and a set of observations that needs confirmation: the $\rho(1570)$, $\rho(1900)$ and $\rho(2150)$ (see Ref. [26]). In the isovector $J^{PC} = 3^{--}$ sector one can expect the production of the well-known and relatively narrow $\rho_3(1690)$ state. At higher energies there have been observations of two $J^{PC} = 3^{--}$ states: the $\rho_3(1990)$ and $\rho_3(2250)$. The first isovector $J^{PC} = 5^{--}$ state is expected to have a mass of around 2350 MeV/c^2. Such a resonance is observed in the analysis of the GAMS2 data for the reaction

$\pi^- p \to \omega\pi^0 n$ [30] and in the analyses of proton-antiproton annihilation in flight into different meson final states (e.g., see Ref. [31]). The decay of the J/ψ through a virtual photon does not forbid but even favors the production of $I^G = 0^-$ resonances. The $J/\psi \to \phi\pi^0$ decay is strongly suppressed [32]; hence the production of excited ϕ mesons is expected to be negligible assuming the absence of strong mixing of excited ϕ and ω states. However, the production of excited ω resonances is possible. The isovector and isoscalar states can be distinguished in a combined analysis of the decay under consideration and the J/ψ decay to $K^\pm K^0\pi^\mp$.

A. Fit to the data

The masses and widths of all states included in the solution [with the sole exception of the $\rho(770)$] are initially free fit parameters. For the well-established $K\pi$ resonances we use results of the LASS fits to the elastic $K\pi$ scattering amplitudes [33] as reference values. The masses and widths of these states are allowed to vary within $\pm\sigma$ of the LASS measurements (here σ stands for the LASS uncertainty). If no NLL minimum is found for the mass or width within this range or the minimum is unstable (with respect to variations of the PWA solution used for estimation of systematic errors), the parameter is set to the central value of the LASS results. Motivated by the claim of an observation of the $K_2^*(1980)^\pm$ by LASS [27] and by Regge trajectories predicting a state at approximately 1.8 GeV/c^2 we introduce a second $J^P = 2^+$ contribution with a mass allowed to vary within the 1.75–2.1 GeV/c^2 interval. Two clear resonancelike K^+K^- signals are found to significantly contribute to the data description in all fits. The first contribution has a mass of around 1.65 GeV/c^2 and is likely a manifestation of the $\rho(1700)$ or $\omega(1650)$, or interference between the two. Note that the parameters of both these states remain highly uncertain. For the $\rho(1700)$, the PDG quotes the results with the mass varying roughly from 1540 to 1860 MeV/c^2, which may indicate the presence of two states. Quark potential models [1] suggest two resonances close to this mass range: 1^3D_1 and 3^3S_1. This possibility is implied in the interpretation of the fit results. The second contribution has a mass of around 2.0–2.1 GeV/c^2, close to the mass of the $\rho(2150)$. No limitations on their parameters are imposed in the fits. For the $\rho(1450)$ the mass range from 1.3 up to 1.5 GeV/c^2 is studied, but no NLL minima are found, and so its mass and width are fixed to the PDG estimates [26].

In the analysis we find that the PWA solution cannot be saturated with well-known states included as Breit-Wigner resonances and constant contributions in the lowest partial waves. At the same time, the "missing part" of the PWA solution cannot be reliably attributed to a single resonance and mainly manifests itself as a slow changing background in the $J^P = 3^-$ partial wave of the $K^\pm\pi^0$ pairs at high $K^\pm\pi^0$ masses. Below we provide two solutions constructed with and without the smooth contribution in this partial wave to demonstrate that the conclusions of this analysis are not strongly affected by assumptions on the "missing part" of the PWA solution.

TABLE I. List of contributions for solution I, showing for each contribution the mass, width, decay fraction and increase in negative log-likelihood for the removal of the state. In the $K\pi$ channel b stands for the decay fraction through both charged conjugated modes and $b^{+(-)}$ gives the contribution of one charged mode, which allows their interference to be determined. The uncertainties are statistical. Parameters marked with * are fixed.

$K^\pm\pi^0$ channels						
J^{PC}	PDG	M (MeV/c^2)	Γ (MeV/c^2)	b (%)	$b^{+(-)}$ (%)	ΔNLL
1^-	$K^*(892)^\pm$	894.1 ± 0.1	46.7 ± 0.2	89.2 ± 0.8	41.0 ± 0.2	...
1^-	$K^*(1680)^\pm$	$1677^\star$	$205^\star$	0.59 ± 0.04	0.25 ± 0.02	398
2^+	$K_2^*(1430)^\pm$	1431.4 ± 0.8	100.3 ± 1.6	9.2 ± 0.1	4.1 ± 0.1	...
2^+	$K_2^*(1980)^\pm$	1817 ± 11	312 ± 28	0.44 ± 0.05	0.17 ± 0.02	238
3^-	$K_3^*(1780)^\pm$	$1781^\star$	$203^\star$	0.08 ± 0.01	0.04 ± 0.01	83
4^+	$K_4^*(2045)^\pm$	2015 ± 7	183 ± 17	0.16 ± 0.02	0.07 ± 0.01	192

K^+K^- channel					
J^{PC}	PDG	M (MeV/c^2)	Γ (MeV/c^2)	b (%)	$\Delta \ln L$
1^{--}	$\rho(770)$	$771^\star$	$150^\star$	1.8 ± 0.2	220
1^{--}	$\rho(1450)$	$1465^\star$	$400^\star$	1.2 ± 0.2	27
1^{--}		1643 ± 3	167 ± 12	1.1 ± 0.1	281
1^{--}		2078 ± 6	149 ± 21	0.15 ± 0.03	73
1^{--}	Nonresonant	...	...	1.2 ± 0.2	34
3^{--}	$\rho_3(1690)$	$1696^\star$	$204^\star$	0.14 ± 0.01	144

B. Solution I

The results for the best fit based on the well-established resonances and constant contributions in the lowest partial waves are given in Table I. Only contributions improving the NLL by more than 17 are included in the fit (corresponding to a statistical significance of 5σ for 4 degrees of freedom). The data description as a Dalitz plot is shown in Fig. 1(b). To evaluate the data description we compute the χ^2-value considering statistical errors only: $\chi^2/NDF = 3314.8/2950$, where NDF stands for the number of degrees of freedom. In this calculation bins with small event number are merged with neighboring ones. Figures 2 and 3 show the corresponding invariant mass spectra and angular distributions. The kinematic distributions in Fig. 3 are restricted to the inner part of the Dalitz plot $[M(K^{\pm}\pi^0) > 1.05\ \mathrm{GeV}/c^2]$ to exclude the huge peaks from the $K^*(892)^{\pm}$.

The dominant contribution stems from the $K^*(892)^{\pm}$ and $K_2^*(1430)^{\pm}$ resonances in the $K^{\pm}\pi^0$ kinematic channels. The first decay is well known and contributes about 90% to the total decay rate. The interference term between the $K^*(892)^+K^-$ and $K^*(892)^-K^+$ intermediate states contributes about 10%. The mass and the width of the $K^*(892)^{\pm}$ are determined with high statistical precision. The Blatt-Weisskopf radius of the resonance is found to be $r = 0.25 \pm 0.02$ fm. The second largest contribution, with a decay fraction of about 10%, is the $K_2^*(1430)^{\pm}$, which also can be clearly seen in Fig. 1. The mass and width of this state are also determined with high precision. Its Blatt-Weisskopf radius cannot be reliably determined from the fit

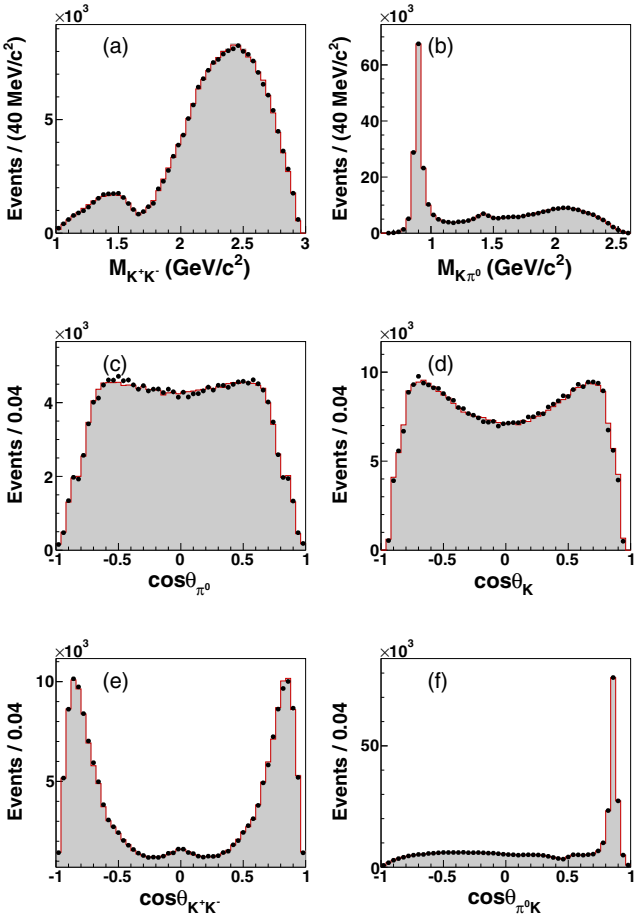

FIG. 2. Kinematical distributions for the data (dots), the PWA solution I (shaded histograms) and the PWA solution II (solid line). The notation K without any specified charge indicates the sum of the K^+ and K^- distributions. (a),(b) Invariant mass of the K^+K^- and $K^{\pm}\pi^0$ systems. (c),(d) Distributions of the final-state particles' polar angle $(\theta_{\pi^0}, \theta_K)$ with respect to the beam axis in the J/ψ rest frame. (e),(f) Polar angle distributions $(\theta_{KK}, \theta_{\pi K})$ for K^+ in the K^+K^- helicity frame (e) and for π^0 in the $K\pi^0$ helicity frame (f). The uncertainties are statistical and are within the size of the dots.

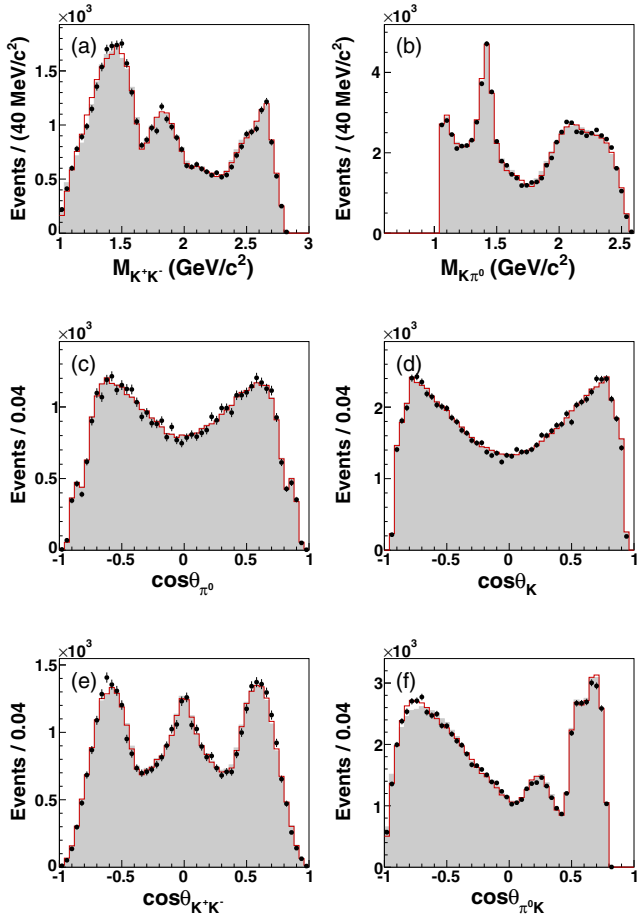

FIG. 3. Kinematical distributions for the data (dots), PWA solution I (shaded histograms) and PWA solution II (solid line) in the inner region of the Dalitz plot $[M(K^{\pm}\pi^0) > 1.05\ \mathrm{GeV}/c^2]$. The notation K without any specified charge indicates the sum of the K^+ and K^- distributions. (a),(b) Invariant mass of the K^+K^- and $K^{\pm}\pi^0$ systems. (c),(d) Distributions of the final-state particles' polar angle $(\theta_{\pi^0}, \theta_K)$ with respect to the beam axis in the J/ψ rest frame. (e),(f) Polar angle distributions $(\theta_{KK}, \theta_{\pi K})$ for K^+ in the K^+K^- helicity frame (e) and for the π^0 in the $K\pi^0$ helicity frame (f). The error bars represent the statistical uncertainties.

and is set to 0.4 fm, which is the meson-interaction radius used in Ref. [29]. The contribution of the $K_2^*(1430)^\pm K^\mp$ channel to the reaction is approximately 10 times smaller than the contribution from the $K^*(892)^\pm K^\mp$ channel. Taking into account this result and using a branching fraction of 49.9% for the $K_2^*(1430)^\pm$ decay to $K\pi$ [26], we find that the J/ψ decay to $K_2^*(1430)^\pm K^\mp$ is suppressed by an approximate factor of 5 compared to the decay to $K^*(892)^\pm K^\mp$. For $J^P = 1^-$, the inclusion of the $K^*(1680)^\pm$ provides a significant improvement in the data description, but no NLL minima consistent with its mass and width are found. The $J^P = 2^+$ partial wave requires another 2^+ state with a relative contribution of approximately 0.4%. Its mass and width are found to be 1817 ± 11 and $312 \pm 28\,\mathrm{MeV}/c^2$, respectively. This mass is much lower than the mass of the $K_2^*(1980)^\pm$ observed by LASS. The $K_3^*(1780)^\pm$ state provides a significant improvement in the log-likelihood, but no NLL minima consistent with its measured parameters are found. Finally, there is a small, but very distinct and stable contribution of $(0.18 \pm 0.02)\%$ from the $K_4^*(2045)^\pm$. Its fitted mass is lower than that obtained in other measurements [26], which can be attributed to the uncertainties of the PWA solution (see solution II).

In the K^+K^- kinematic channel, the first stable contribution has $J^{PC} = 1^{--}$, a mass of $1643 \pm 3\ \mathrm{MeV}/c^2$, a width of $167 \pm 12\ \mathrm{MeV}/c^2$ and a decay fraction of 1%. It can also be clearly seen in the Dalitz plot. As mentioned above, this contribution can be attributed to the $\rho(1700)$. The structure is also reasonably consistent with the $\omega(1650)$ (the mass is consistent with the PDG estimate, and the width is well within the spread of the results quoted by PDG) or an interference between these states. The second contribution that can be reliably determined from the data is a $J^{PC} = 1^{--}$ resonance with a mass of $2078 \pm 6\ \mathrm{MeV}/c^2$ and width of $149 \pm 21\ \mathrm{MeV}/c^2$. The largest relative contribution of $(1.8 \pm 0.2)\%$ comes from the tail of the $\rho(770)$. Since the mass of this state is significantly below the K^+K^- production threshold, no reliable claim can be made about its observation. The $\rho_3(1690)$ and $\rho(1450)$ provide NLL improvement by 144 and 27, but no NLL minimum consistent with the parameters of each state is found. The smooth contribution in the $J^{PC} = 1^{--}$ K^+K^- partial wave is also found to be significant.

Additionally, we try to set the mass and the width of the $J^{PC} = 1^{--}$ K^+K^- contribution at 1.65 GeV/c^2 to the PDG mean values for the $\rho(1700)$ averaged from $\eta\rho(770)$ and $\pi^+\pi^-$ modes. In this case, the NLL worsens by 42, and so one may consider including the $\omega(1420)$ and $\omega(1650)$ in the fit. In these fits we set their masses and width to the mean values of the PDG estimates. If the $\omega(1420)$ [$\omega(1650)$] is included, the NLL is still worse by 14 (7) compared to the result of solution I. If the $\rho(1450)$ is substituted by the $X(1575)$, instead of adding a resonance, the NLL improves by 28, but remains worse by 14 than the result for solution I.

Adding further well-established resonances with the nominal PDG parameters does not improve log-likelihood by more than 17 units. Despite this, the solution is not saturated: if additional contributions (parametrized as Breit-Wigner resonances with parameters not required to correspond to a physical state) are added, they can improve NLL by up to 95 in a single partial wave, which is much larger than the contribution of other resonances included in the solution. The only notable additional contribution indicating resonance behavior is in the $J^P = 1^-$ $K\pi$ partial wave with a mass of around 2.4 GeV/c^2, but there is a lack of qualitative evidence to report a new state. The largest improvement in the NLL function comes from contributions that tend to be broad and cannot be interpreted as resonances. These conclusions are not surprising if one considers the measured two-particle $K\pi$ scattering amplitudes obtained by the LASS Collaboration [33]. Here the F-wave intensity, apart from the $K_3^*(1780)$ peak, has a strong contribution from nontrivial structures, which are not resolved in the LASS analysis. The inability to provide a consistent data description for this solution prevents us from making a reliable estimation of systematic uncertainties.

C. Solution II

We find that the largest improvement to the NLL of solution I comes from the inclusion of a smooth contribution in the $J^P = 3^-$ partial wave, which we parametrize with a broad Breit-Wigner shape. Its mass is found to be close to the maximal allowed invariant mass of the $K^\pm\pi^0$ system. The width can vary in the approximate interval of 0.5–1.2 GeV/c^2, depending on small variations of the PWA solution, and its value only slightly affects other components in the fit. Such a mass and width does not allow an interpretation of this contribution as a single resonance. The solution where this broad component is added and the significance of the resonances is reevaluated is shown in Table II. For this solution, we use the more conservative resonance significance criteria: the minimum NLL improvement is required to be 40. We ensure that no other allowed resonance contributions improve the NLL value above this number, considering possibilities with spins up to $J = 5$, which is the maximum spin of previously reported states allowed in this decay. Those contributions which give the most significant NLL improvement are used to estimate systematic uncertainties. The NLL value for this solution is better by 116 than that of solution I. The systematic uncertainties listed in Table II will be discussed later. The Dalitz plot for solution II is shown in Fig. 1(c). If it is compared to the Dalitz plot for the data in the same way as for solution I, one gets $\chi^2/NDF = 3191.0/2950$. Mass and angular distributions are given in Figs. 2 and 3 for the data and for the two models. The two descriptions are very

TABLE II. List of components for solution II. For the reported states in the $K\pi$ channel [$K^*(892)^\pm$, $K_2^*(1430)^\pm$, $K_2^*(1980)^\pm$ and $K_4^*(2045)^\pm$] and the reported signals in the K^+K^- channel ($J^{PC}=1^{--}$ signals with masses around 1650 and 2050 MeV/c^2) the first uncertainty is statistical and the second is systematic. In the $K\pi$ channel the decay fraction is given for both charged conjugated modes (b) and for the contribution of one charged mode [$b^{+(-)}$], so that their interference can be determined. As the $K^*(1410)^\pm$, $K^*(1680)^\pm$ and $K_3^*(1780)^\pm$ contributions are not reliably identified (see the main text), their masses and widths are fixed (marked with *) and only statistical uncertainties are given for their decay fractions.

$K^\pm\pi^0$ channels

J^{PC}	PDG	M (MeV/c^2)	Γ (MeV/c^2)	b (%)	$b^{+(-)}$ (%)	ΔNLL
1^-	$K^*(892)^\pm$	$893.6\pm0.1^{+0.2}_{-0.3}$	$46.7\pm0.2^{+0.1}_{-0.2}$	$93.4\pm0.4^{+1.8}_{-5.8}$	$42.5\pm0.1^{+0.5}_{-1.7}$	...
1^-	$K^*(1410)^\pm$	$1380^\star$	$176^\star$	0.26 ± 0.04	0.11 ± 0.02	80
1^-	$K^*(1680)^\pm$	$1677^\star$	$205^\star$	0.20 ± 0.03	0.08 ± 0.01	56
2^+	$K_2^*(1430)^\pm$	$1432.7\pm0.7^{+2.2}_{-2.3}$	$102.5\pm1.6^{+3.1}_{-2.8}$	$9.4\pm0.1^{+0.8}_{-0.5}$	$4.2\pm0.1^{+0.3}_{-0.2}$	...
2^+	$K_2^*(1980)^\pm$	$1868\pm8^{+40}_{-57}$	$272\pm24^{+50}_{-15}$	$0.38\pm0.04^{+0.22}_{-0.05}$	$0.15\pm0.02^{+0.08}_{-0.02}$	192
3^-	$K_3^*(1780)^\pm$	$1781^\star$	$203^\star$	0.16 ± 0.02	0.07 ± 0.01	105
4^+	$K_4^*(2045)^\pm$	$2090\pm9^{+11}_{-29}$	$201\pm19^{+57}_{-17}$	$0.21\pm0.02^{+0.10}_{-0.05}$	$0.09\pm0.01^{+0.04}_{-0.02}$	212
3^-	Nonresonant	...	...	~1.5%	~0.6%	629

K^+K^- channel

J^{PC}	PDG	M (MeV/c^2)	Γ (MeV/c^2)	b (%)	$\Delta \ln L$
1^{--}		$1651\pm3^{+16}_{-6}$	$194\pm8^{+15}_{-7}$	$1.83\pm0.11^{+0.19}_{-0.17}$	796
1^{--}		$2039\pm8^{+36}_{-18}$	$196\pm23^{+25}_{-27}$	$0.23\pm0.04^{+0.07}_{-0.06}$	102

similar, but solution II is superior in specific kinematic regions.

Solution II has the same set of well-defined contributions as solution I. The fitted mass and width for the $K^*(892)^\pm$ and $K_2^*(1430)^\pm$ are almost the same. The mass, width and Blatt-Weisskopf radius of the $K^*(892)$ are found to be $M=893.6\pm0.1^{+0.2}_{-0.3}$ MeV/c^2, $\Gamma=46.7\pm0.2^{+0.1}_{-0.2}$ MeV/c^2 and $r=0.20\pm0.02^{+0.14}_{-0.04}$ fm, respectively, where here and subsequently the first uncertainty is statistical, and the second is systematic. The mass lies between the PDG averages for measurements performed where the $K^*(892)^\pm$ is produced in hadronic collisions and those where it is produced in τ decays [26]. The fitted width is consistent with the τ-decay results [34]. For the $K_2^*(1430)^\pm$ we fix the Blatt-Weisskopf radius to 0.4 fm. The 2^+ partial amplitude in the $K^\pm\pi^0$ kinematic channels also requires a second contribution with a mass higher than that of the previous solution with large systematic uncertainties for both the mass and width: $M=1868\pm8^{+40}_{-57}$ MeV/c^2 and $\Gamma=272\pm24^{+50}_{-15}$ MeV/c^2. The mass is approximately 100 MeV/c^2 below the LASS measurement for the $K_2^*(1980)$ [27], but both the mass and the width are compatible with the PDG averages within 2.2 standard deviations. As in solution I, there is a very clear contribution to the $J^P=4^+$ partial wave with $M=2090\pm9^{+11}_{-29}$ MeV/c^2 and $\Gamma=201\pm19^{+57}_{-17}$ MeV/c^2, which is consistent with the parameters of the $K_4^*(2045)^\pm$ [26]. For the $K^*(1410)$, which is required in this solution; the $K^*(1680)^\pm$; and the $K_3^*(1780)^\pm$, no NLL minima consistent with parameters of these resonances are found. In the K^+K^- kinematic channel we see again two stable contributions at 1.65 and 2.05 GeV/c^2. The contributions from the $\rho(1450)$, $\rho_3(1690)$ and $\rho(770)$ are marginal.

A striking feature of solution II is the presence of a nonresonance component in the $J^P=3^-$ $K^\pm\pi^0$ partial waves, which cannot be clearly interpreted as an interference between Breit-Wigner states. A possible interpretation is that this component is the manifestation of nonresolved contributions present in the F-wave $K\pi$ scattering amplitude [33]. This may include the presence of several resonances, nonresonant production and final-state particle rescattering effects.

The stability of the found NLL minimum with respect to the parameters of the reported resonances is demonstrated in Fig. 4.

The systematic errors due to the uncertainty of the PWA solution are assigned to be the largest deviations for the following variations of the solution:

(i) Variation of the masses and widths for the $K^\pm\pi^0$ resonances with the parameters fixed in the fit, and varied by one standard deviation of the LASS results [33];
(ii) Variation of the Blatt-Weisskopf radius of the $K_2^*(1430)^\pm$ by ±0.2 fm;
(iii) Inclusion of contributions that strongly improve the log-likelihood below the acceptance criteria [$J^P=1^-$ $(K\pi)$ at approximately 2.5 GeV/c^2 and $J^{PC}=1^{--}$ (K^+K^-) at $M(K^+K^-)\approx2.3$ GeV/c^2];

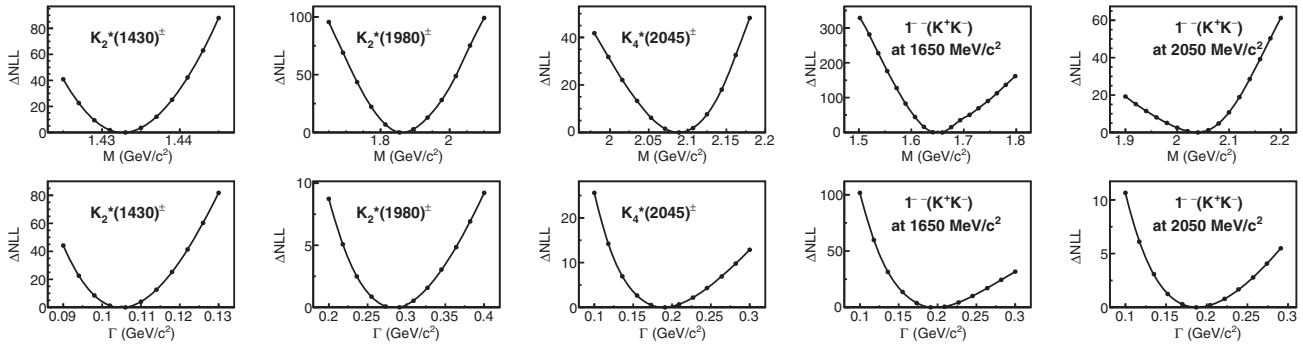

FIG. 4. Mass and width scans for the $K_2^*(1430)$, $K_2^*(1980)$, $K_4^*(2045)$ and 1^{--} structures at 1650 and 2050 MeV$/c^2$ for solution II.

(iv) Reparametrization of the broad background part of partial waves.

To evaluate the latter variation, broad contributions in the 1^-, 2^+ $(K\pi)$ amplitudes and 1^{--} (K^+K^-) partial wave parametrized with $\rho(770)^0$ and $\rho(1450)^0$ are studied. In all these fits the states $K^*(892)^\pm$, $K_2^*(1430)^\pm$, $K_4^*(2045)^\pm$ and the structures at 1.65 and 2.05 GeV$/c^2$ in the K^+K^- channels remain stable. The high-mass broad $K^\pm\pi^0$ 3^- contribution always remains significant, but its relative fraction varies to much smaller values in some fits. The 1^- additional contribution mostly manifests resonant behavior. No stable contribution can be associated with the $\rho(1450)$, but its relative decay fraction at the level of 1% does not contradict the data.

The total systematic uncertainties for the masses, widths and decay fraction given in Table II are calculated as a quadratic sum of

(i) The variation in results due to the uncertainty of the PWA solution;
(ii) The bias introduced by imperfections of the detector simulation and the event reconstruction;
(iii) The uncertainties due to the differences in kaon tracking and PID efficiencies between data and the MC simulation.

The differences in kaon tracking and PID efficiencies between data and the MC simulation are studied with a high-purity control sample of $J/\psi \to K_S K^\pm\pi^\mp$ decays as a function of kaon transverse momentum p_T and are found to be within 1% per track both for the tracking and the PID. The effect on the PWA result is estimated by varying the selection efficiency difference for data and MC in p_T bins within these errors. Uncertainties on the fit parameters due to the efficiency variation in each bin are summed quadratically.

The background uncertainty, estimated by varying the subtracted NLL contribution by 50%, is found to be negligible.

D. Summary on PWA

Our analysis shows that there is a set of states in the PWA solutions that remains stable for both considered cases: when contributions corresponding to well-known resonances are considered or when broad contributions are introduced to parametrize the missing part of the partial amplitudes. In the $K^\pm\pi^0$ channels this set of resonances includes the $K^*(892)^\pm$, $K_2^*(1430)^\pm$, and $K_4^*(2045)^\pm$. The second $J^P = 2^+$ state, labeled here as $K_2^*(1980)^\pm$, has a mass much lower than that observed by the LASS Collaboration [27]. However, given the large systematic uncertainties on this quantity, our result is compatible within 2.2 standard deviations. The first stable structure in the K^+K^- channel has a mass of about 1.65 GeV$/c^2$ and a decay fraction of 1.0%–1.5%. The absence of a distinct contribution from the first radial excitation of the $\rho(770)$ favors its interpretation as a $^3D_1$ ρ-resonance. At the same time such a small decay fraction is consistent with $\omega(1650)$ production in J/ψ decay through a virtual photon. Its mass is consistent with the PDG estimate for the $\omega(1650)$ and its width is well within the spread of experimental results quoted by the PDG. It could also be the result of interference between these isovector and isoscalar states. The second stable contribution has a mass of about 2.05–2.10 GeV$/c^2$ and decay fraction of 0.1%–0.2%. Given the large systematic uncertainties it could be interpreted as either the $\rho(2150)$ or as another isovector-vector state observed in proton-antiproton annihilation in flight [35]. Clarification of the nature of these excited vector mesons requires further investigation.

V. BRANCHING FRACTIONS

The $J/\psi \to K^+K^-\pi^0$ branching fraction is determined as $B(J/\psi \to K^+K^-\pi^0) = \frac{N_{\rm sel} - N_{\rm bg} - N_{\rm continuum}}{\epsilon N_{J/\psi} B(\pi^0 \to \gamma\gamma)}$. Here $N_{\rm sel}$, $N_{\rm bg}$ and $N_{\rm continuum}$ are the number of selected events, the estimated background from the J/ψ decays, and the continuum production, respectively. The number of J/ψ events $N_{J/\psi} = (223.7 \pm 1.4({\rm syst})) \times 10^6$ is taken from Ref. [13], and $B(\pi^0 \to \gamma\gamma) = (98.823 \pm 0.034) \times 10^{-2}$ is taken from the PDG [26]. The selection efficiency ϵ is obtained using the PWA solution II and the detector performance simulation. The dominant contribution to the statistical uncertainty comes from $N_{\rm sel}$. The systematic

TABLE III. Summary of systematic uncertainties for $B(J/\psi \to K^+K^-\pi^0)$.

Source	Uncertainty (%)
$N_{\rm bg}$	0.2
$N_{\rm continuum}$	0.3
Track reconstruction efficiency	2.0
PID efficiency	2.0
Photon reconstruction efficiency	2.0
Kinematic fit cut efficiency	2.4
$N_{J/\psi}$ [13]	0.6
Total	4.3

uncertainty on the branching fraction is estimated from the sources listed in Table III. The background uncertainty is estimated by varying N_{bg} by $\pm 50\%$. The uncertainty associated with the subtraction of the continuum background is assigned to be the statistical error on $N_{\rm continuum}$. The charged track reconstruction efficiency and the PID efficiency uncertainties are 1% each per track as is discussed above. The photon detection efficiency is studied with the decays $\psi(3686) \to \pi^+\pi^- J/\psi$, $J/\psi \to \rho^0\pi^0$ and photon conversion control samples [36,37]. In this analysis, an uncertainty of 1% per photon is assigned. The uncertainty introduced by the cut on $\chi^2_{K^+K^-\gamma\gamma}$ is estimated using a control sample. This is selected using similar selection criteria, with the kinematic-fit cut replaced by the requirement that at least one particle out of three (K^+, K^-, π^0) have a mass hypothesis consistent with the recoil mass calculated using the other two particles. Such a procedure accepts a signal event even if one of the particles is badly reconstructed. This gives $B(J/\psi \to K^+K^-\pi^0) = (2.88 \pm 0.01 \pm 0.12) \times 10^{-3}$.

Knowing the $J/\psi \to K^+K^-\pi^0$ branching fraction and the decay fractions for the individual components from the PWA, we determine branching fractions for the decay via individual resonances. Results for solution II are summarized in Table IV. The branching fraction $B(J/\psi \to K^+K^-\pi^0)$ and the branching fractions for the decay via the $K^*(892)^\pm$ that are obtained in solution II are compared to the results from previous experiments in Table V. Our result for $B(J/\psi \to K^+K^-\pi^0)$ is up to now the most precise measurement. It differs from the PDG value [26], obtained indirectly from Ref. [11], by about a 2.8 standard deviation. The systematic uncertainty of our results for decays through

TABLE IV. Branching fractions for decays via reliably identified intermediate states (solution II). $R_{K\pi}$ and R_{KK} denote $K^\pm\pi^0$ and K^+K^- resonances, respectively, and $R^\pm_{K\pi}K^\mp$ denotes one possible charged combination. The first uncertainty is statistical and the second one is systematic.

Intermediate resonance in the $K\pi$ system		
$R_{K\pi}$	$B(J/\psi \to R^\pm_{K\pi}K^\mp \to K^+K^-\pi^0)$	$B(J/\psi \to R^+_{K\pi}K^- + \text{c.c.} \to K^+K^-\pi^0)$
$K^*(892)$	$(1.22 \pm 0.01^{+0.05}_{-0.07}) \times 10^{-3}$	$(2.69 \pm 0.01^{+0.13}_{-0.20}) \times 10^{-3}$
$K^*_2(1430)$	$(1.21 \pm 0.02^{+0.10}_{-0.08}) \times 10^{-4}$	$(2.69 \pm 0.04^{+0.25}_{-0.19}) \times 10^{-4}$
$K^*_2(1980)$	$(4.3 \pm 0.5^{+2.3}_{-0.6}) \times 10^{-6}$	$(1.1 \pm 0.1^{+0.6}_{-0.1}) \times 10^{-5}$
$K^*_4(2045)$	$(2.6 \pm 0.3^{+1.1}_{-0.6}) \times 10^{-6}$	$(6.2 \pm 0.7^{+2.8}_{-1.4}) \times 10^{-6}$
Intermediate resonance in the K^+K^- system		
R_{KK}		$B(J/\psi \to R_{KK}\pi^0 \to K^+K^-\pi^0)$
$1^{--}(1650\ \text{MeV}/c^2)$		$(5.3 \pm 0.3^{+0.6}_{-0.5}) \times 10^{-5}$
$1^{--}(2050\ \text{MeV}/c^2)$		$(6.7 \pm 1.1^{+2.2}_{-1.8}) \times 10^{-6}$

TABLE V. Comparison between this work and previous measurements. For $B(J/\psi \to K^{*+}K^- + \text{c.c.} \to K^+K^-\pi^0)$ and $B(J/\psi \to K^{*+}K^- + \text{c.c.})$ we give two numbers for solution II: the first one is a sum of branching fractions through K^{*+} and K^{*-} and the second number (in parenthesis) accounts for their interference. Results marked with the † symbol are obtained by averaging the $K_S K^\pm\pi^\mp$ and $K^+K^-\pi^0$ final states. Results recalculated by us using numbers from this work are marked with the †† symbol.

	$B(\times 10^{-3})$				
Channel	This work	*BABAR* [11]	DM2 [9]	MARK-III [8]	MARK-II [7]
$B(J/\psi \to K^+K^-\pi^0)$	$2.88 \pm 0.01 \pm 0.12$	...	...	...	2.8 ± 0.8
$B(J/\psi \to K^{*+}K^- + \text{c.c.} \to K^+K^-\pi^0)$	$2.45 \pm 0.01^{+0.10}_{-0.14}\ (2.69 \pm 0.01^{+0.13}_{-0.20})$	$1.97 \pm 0.16 \pm 0.13$	$1.50 \pm 0.23 \pm 0.27^{\dagger\dagger}$	$1.87 \pm 0.04 \pm 0.28^{\dagger\dagger}$	2.6 ± 0.8
$B(J/\psi \to K^{*+}K^- + \text{c.c.})$	$7.34 \pm 0.03^{+0.33}_{-0.43}\ (8.07 \pm 0.04^{+0.38}_{-0.61})$	$5.2 \pm 0.3 \pm 0.2^\dagger$	$4.57 \pm 0.17 \pm 0.70^\dagger$	$5.26 \pm 0.13 \pm 0.53^\dagger$	$7.8 \pm 2.4^{\dagger\dagger}$

the $K^*(892)^\pm$ is somewhat larger than that of Ref. [11], which can be attributed to the uncertainties present in the PWA model.

VI. CONCLUSION

A partial-wave analysis of the decay $J/\psi \to K^+K^-\pi^0$ using a data sample of $(223.7 \pm 1.4) \times 10^6$ J/ψ events collected by the BESIII reveals a set of resonances that have not been observed by previous experiments. In the $K^\pm\pi^0$ channels our analysis reveals signals from $K_2^*(1980)^\pm$ and $K_4^*(2045)^\pm$ resonances. This is the first observation of these states in J/ψ decays. The mass of the former state is determined with a central value around 100 MeV/c^2 lower than that reported by the LASS Collaboration [29]. This lower value is in better agreement with the expectation from the linear Regge trajectory of radial excitations with the standard slope [38]. As for the known decays through $K\pi$ resonances, we determine the parameters, decay ratios, and branching fractions for the $K^*(892)^\pm$ and $K_2^*(1430)^\pm$ with improved precision compared to previous measurements. In the K^+K^- channel we observe a clear $J^{PC} = 1^{--}$ resonance structure with a mass of 1.65 GeV/c^2 and another $J^{PC} = 1^{--}$ contribution at 2.05–2.10 GeV/c^2. The first structure may be interpreted as the ground $^3D_1$ isovector state. At the same time its mass, width and small relative contribution to the decay are reasonably consistent with the production of the $\omega(1650)$ in J/ψ decays through a virtual photon. The second state can be interpreted as the $\rho(2150)$ or as another isovector-vector state that has been observed in proton-antiproton annihilation in flight [35]. The precise identification of these two states requires further analysis of more channels, such as $J/\psi \to K_S K^\pm\pi^\mp$ and $J/\psi \to K^+K^-\eta$. In this analysis we also report the most precise measurement of the branching fraction $B(J/\psi \to K^+K^-\pi^0)$. Our PWA solutions have notable differences from those presented in Ref. [10] and more recently in Ref. [12]. In particular, we observe only marginal hints for the $K^*(1410)^\pm$, do not observe the large production rate of $X(1575)$ reported in Ref. [10], and are unable to reliably identify the $\rho(1450)$.

ACKNOWLEDGMENTS

The BESIII Collaboration thanks the staff of BEPCII and the IHEP computing center for their strong support. This work is supported in part by National Key Basic Research Program of China under Contract No. 2015CB856700; National Natural Science Foundation of China (NSFC) under Contracts No. 11625523, No. 11635010, and No. 11735014; National Natural Science Foundation of China (NSFC) under Contract No. 11835012; the Chinese Academy of Sciences (CAS) Large-Scale Scientific Facility Program; Joint Large-Scale Scientific Facility Funds of the NSFC and CAS under Contracts No. U1532257, No. U1532258, No. U1732263, and No. U1832207; CAS Key Research Program of Frontier Sciences under Contracts No. QYZDJ-SSW-SLH003 and No. QYZDJ-SSW-SLH040; 100 Talents Program of CAS; INPAC and Shanghai Key Laboratory for Particle Physics and Cosmology; German Research Foundation DFG under Contract No. Collaborative Research Center CRC 1044; DFG and NSFC (CRC 110); Istituto Nazionale di Fisica Nucleare, Italy; Koninklijke Nederlandse Akademie van Wetenschappen (KNAW) under Contract No. 530-4CDP03; Ministry of Development of Turkey under Contract No. DPT2006K-120470; the National Science and Technology fund; the Knut and Alice Wallenberg Foundation (Sweden) under Contract No. 2016.0157; the Royal Society, UK under Contract No. DH160214; the Swedish Research Council; the U.S. Department of Energy under Contracts No. DE-FG02-05ER41374, No. DE-SC-0010118, and No. DE-SC-0012069; the University of Groningen (RuG) and the Helmholtzzentrum fuer Schwerionenforschung GmbH (GSI), Darmstadt. This paper is also supported by the NSFC under Contract No. 10805053.

[1] S. Godfrey and N. Isgur, Phys. Rev. D **32**, 189 (1985).
[2] A. V. Anisovich, V. V. Anisovich, and A. V. Sarantsev, Phys. Rev. D **62**, 051502(R) (2000).
[3] S. Afonin and I. Pusenkov, Phys. Lett. B **726**, 283 (2013).
[4] S. S. Afonin and I. V. Pusenkov, Phys. Rev. D **90**, 094020 (2014).
[5] E. Klempt and A. Zaitsev, Phys. Rep. **454**, 1 (2007).
[6] F. Vannucci, M. S. Alam, A. M. Boyarski, M. Breidenbach, G. J. Feldman, D. Fryberger, F. J. Gilman, G. Hanson, J. A. Jaros *et al.*, Phys. Rev. D **15**, 1814 (1977).
[7] M. Franklin, G. Feldman, G. Abrams, M. Alam, C. Blocker *et al.*, Phys. Rev. Lett. **51**, 963 (1983).
[8] D. Coffman *et al.* (MARK-III Collaboration), Phys. Rev. D **38**, 2695 (1988).
[9] J. Jousset, Z. Ajaltouni, A. Falvard, H. Jnad, B. Michel, J. C. Montret, D. Bisello, G. Busetto, A. Castro *et al.* (DM2 Collaboration), Phys. Rev. D **41**, 1389 (1990).
[10] M. Ablikim *et al.* (BES Collaboration), Phys. Rev. Lett. **97**, 142002 (2006).

[11] B. Aubert *et al.* (*BABAR* Collaboration), Phys. Rev. D **77**, 092002 (2008).
[12] J. P. Lees *et al.* (*BABAR* Collaboration), Phys. Rev. D **95**, 072007 (2017).
[13] M. Ablikim *et al.* (BESIII Collaboration), Chin. Phys. C **41**, 013001 (2017).
[14] M. Ablikim *et al.* (BESIII Collaboration), Nucl. Instrum. Methods Phys. Res., Sect. A **614**, 345 (2010).
[15] C. Yu *et al.*, in *Proc. of International Particle Accelerator Conference (IPAC'16), Busan, Korea, 2016*, International Particle Accelerator Conference No. 7 (JACoW, Geneva, Switzerland, 2016), pp. 1014–1018.
[16] Z. Y. Deng *et al.*, High Energy Phys. Nucl. Phys. **30**, 371 (2006).
[17] S. Jadach, Comput. Phys. Commun. **130**, 244 (2000).
[18] S. Jadach, B. F. L. Ward, and Z. Was, Phys. Rev. D **63**, 113009 (2001).
[19] D. Lange, Nucl. Instrum. Methods Phys. Res., Sect. A **462**, 152 (2001).
[20] R.-G. Ping, Chin. Phys. C **32**, 599 (2008).
[21] C. Amsler *et al.* (Particle Data Group), Phys. Lett. B **667**, 1 (2008).
[22] J. C. Chen, G. S. Huang, X. R. Qi, D. H. Zhang, and Y. S. Zhu, Phys. Rev. D **62**, 034003 (2000).
[23] B. Zou and D. Bugg, Eur. Phys. J. A **16**, 537 (2003).
[24] D. V. Bugg, I. Scott, B. S. Zou, V. V. Anisovich, A. V. Sarantsev, T. H. Burnett, and S. Sutlief, Phys. Lett. B **353**, 378 (1995).
[25] I. Denisenko and I. Boyko, J. Instrum. **10**, P10028 (2015).
[26] M. Tanabashi *et al.* (Particle Data Group), Phys. Rev. D **98**, 030001 (2018).
[27] D. Aston, N. Awaji, J. D'Amore, W. Dunwoodie, R. Endorf *et al.*, Nucl. Phys. **B292**, 693 (1987).
[28] G. D. Tikhomirov, I. A. Erofeev, O. N. Erofeeva, and V. N. Luzin, Phys. At. Nucl. **66**, 828 (2003).
[29] D. Aston, N. Awaji, J. D'Amore, W. Dunwoodie, R. Endorf *et al.*, Phys. Lett. B **180**, 308 (1986).
[30] D. Alde *et al.* (GAMS Collaboration), Il Nuovo Cimento A **107**, 1867 (1994).
[31] A. V. Anisovich, C. A. Baker, C. J. Batty, D. V. Bugg, L. Montanet, V. A. Nikonov, A. V. Sarantsev, V. V. Sarantsev, and B. S. Zou, Phys. Lett. B **542**, 8 (2002).
[32] M. Ablikim *et al.* (BESIII Collaboration), Phys. Rev. D **91**, 112001 (2015).
[33] D. Aston, N. Awaji, T. Bienz, F. Bird, J. D'Amore *et al.*, Nucl. Phys. **B296**, 493 (1988).
[34] D. Epifanov *et al.* (Belle Collaboration), Phys. Lett. B **654**, 65 (2007).
[35] A. V. Anisovich, C. A. Baker, C. J. Batty, D. V. Bugg, C. Hodd, H. C. Lu, V. A. Nikonov, A. V. Sarantsev, V. V. Sarantsev, and B. S. Zou, Phys. Lett. B **491**, 47 (2000).
[36] M. Ablikim *et al.* (BESIII Collaboration), Phys. Rev. D **81**, 052005 (2010).
[37] M. Ablikim *et al.* (BESIII Collaboration), Phys. Rev. D **83**, 112005 (2011).
[38] V. V. Anisovich, AIP Conf. Proc. **619**, 197 (2002).